

Soldering-based easy packaging of thin polyimide multichannel electrodes for neuro-signal recording

This article has been downloaded from IOPscience. Please scroll down to see the full text article.

2012 J. Micromech. Microeng. 22 115017

(<http://iopscience.iop.org/0960-1317/22/11/115017>)

View [the table of contents for this issue](#), or go to the [journal homepage](#) for more

Download details:

IP Address: 166.104.29.37

The article was downloaded on 10/10/2012 at 12:32

Please note that [terms and conditions apply](#).

Soldering-based easy packaging of thin polyimide multichannel electrodes for neuro-signal recording

Dong-Hyun Baek^{1,2}, Chang-Hee Han³, Ha-Chul Jung¹, Seon Min Kim¹,
Chang-Hwan Im³, Hyun-Jik Oh⁴, James Jungho Pak²
and Sang-Hoon Lee¹

¹ Department of Biomedical Engineering, College of Health Science, Korea University, Seoul 136-703, Korea

² School of Electrical Engineering, Korea University, Anam-dong, Seongbuk-gu, Seoul, Korea

³ Department of Biomedical Engineering, Hanyang University, Seoul, Korea

⁴ MicroFIT Co. Ltd, College of Health Science, Korea University, Seoul 136-703, Korea

E-mail: dbiomed@korea.ac.kr and pak@korea.ac.kr

Received 25 July 2012

Published 26 September 2012

Online at stacks.iop.org/JMM/22/115017

Abstract

We propose a novel packaging method for preparing thin polyimide (PI) multichannel microelectrodes. The electrodes were connected simply by making a via-hole at the interconnection pad of a thin PI electrode, and a nickel (Ni) ring was constructed by electroplating through the via-hole to permit stable soldering with strong adhesion to the electrode and the printed circuit board. The electroplating conditions were optimized for the construction of a well-organized Ni ring. The electrical properties of the packaged electrode were evaluated by fabricating and packaging a 40-channel thin PI electrode. Animal experiments were performed using the packaged electrode for high-resolution recording of somatosensory evoked potential from the skull of a rat. The *in vivo* and *in vitro* tests demonstrated that the packaged PI electrode may be used broadly for the continuous measurement of bio-signals or for neural prosthetics.

 Online supplementary data available from stacks.iop.org/JMM/22/115017/mmedia

(Some figures may appear in colour only in the online journal)

1. Introduction

The interception and recording of electrical impulses from biological tissues or the stimulation of nerve systems with high spatio-temporal resolution is a hot issue in neuroprosthetic research. A central goal is to restore or assist in the recovery of lost sensory or motor function via man-machine interfaced robotics [1–3]. In living creatures, neurons are polarized by the membrane transport proteins, and the electric signals (e.g. electroencephalography (EEG) or evoked potentials) from the brain are generated by the intricately networked neurons and they provide important information of brain activity. The measurement of the electric signal from the networked neurons with minimal noise and fine spatiotemporal resolution

is critical in diagnosis and the brain-computer interface. For this purpose, the development and packaging of multiple microelectrode arrays (MMEAs) and recording of populated neural activity as precisely as possible are highly required. To date, several micro-sized multichannel electrodes have been developed, including electrodes penetrated to targeted regions and contact the cortical cortex or skull. Polyimide (PI) has been mostly used as a substrate due to its excellent thermal stability, high chemical resistance and ability to form thin and flexible films that can be patterned using photolithography processes [4–6]. Although the PI MMEA technology has progressed rapidly, the practical applications of these electrodes are limited by their packaging technologies, particularly with respect to system interconnections. The thickness of a PI

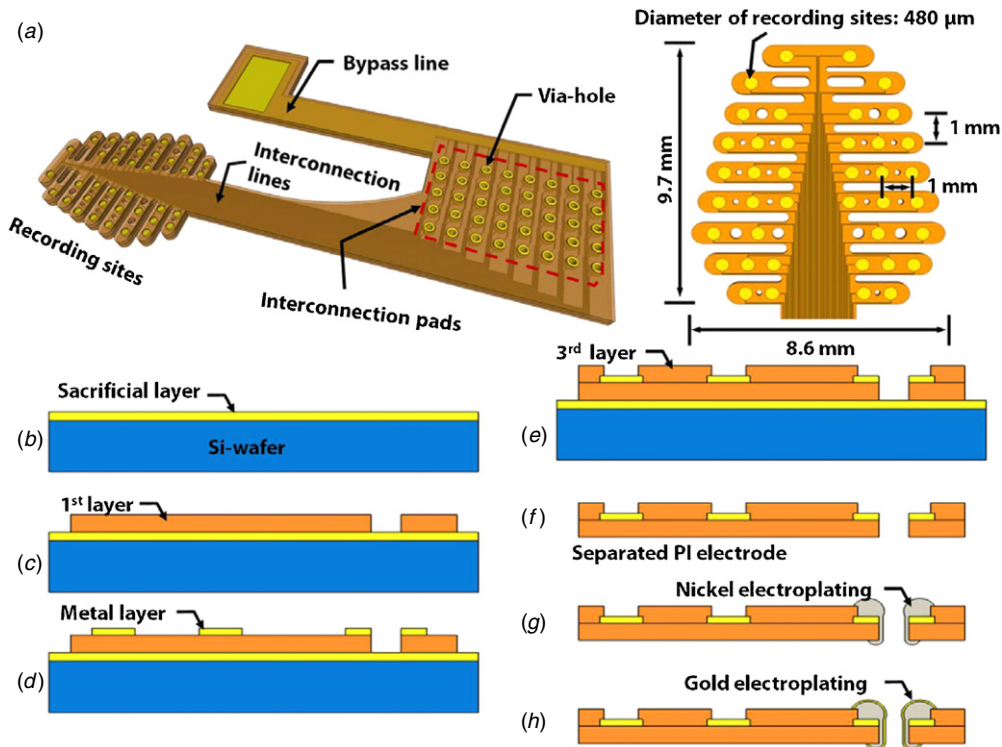


Figure 1. Schematic diagram of the 40-channel microelectrode's fabrication process via photolithography. (a) The interconnection pad was electroplated with nickel and gold. (b) The sacrificial layer deposition. (c) The PI layer (first layer) patterning. (d) The metal layers (second layer) deposition and the second (Ti/Au) layers patterning. (e) The PI layer (third layer) patterning. (f) Separation of the PI electrode. (g) The interconnection pads were electroplated with nickel. (h) A gold layer was electroplated.

electrode is about $10\ \mu\text{m}$; it is, therefore, challenging to develop mechanically stable simple packaging methods. Besides, it is still challenging to maintain stable connection for the neurophysiological experiment using small and free-moving animals due to difficulty in fixation of a connector without mechanical failure. To date, several materials and methods have been reported as a useful connecting method of MMEA [5–7], including soldering paste [8], conductive epoxy adhesives [9, 10] or zero-insertion-force (ZIF) connectors [11, 12]. Although these packaging technologies are useful and ingenious, they still have limitations in practical use due to high costs, high degree of skill or labor-intensiveness, and the reliability and robustness of packaging technology is still challenging. Recently, we developed an anisotropic conductive film (ACF)-based adhesion method for use in preparing MMEAs [13]. The bonding process is parallel, simple, rapid and easy; however, high temperatures and pressures, which must be applied directly to the thin metal pattern on PI for a few tens of seconds [14], can occasionally damage the thin film electrode.

In this paper, we develop a stable, highly yieldable, solderable and cost-effective packaging method for thin flexible MMEAs. Simple connections were implemented by making via-holes at the interconnection pad between the thin PI electrodes with a soldering process. The electroplated Ni ring through the via-hole was constructed to achieve stable soldering and strong adhesion of the electrode to the printed circuit board (PCB). The electroplating conditions for the well-organized Ni ring were optimized, and the electrical properties

of the packaged electrode were evaluated. A 40-channel thin PI electrode was fabricated and packaged using the proposed method, and we evaluated this packaged electrode for use in high-resolution recording of neural signals from the skull of a rat.

2. Materials and method

2.1. Design and fabrication of the polyimide electrode

Figure 1(a) illustrates a schematic diagram showing a 40-channel microelectrode fabricated using photolithography techniques. The interconnection pad was electroplated with nickel and gold. PI (Durimide 7505TM, Fuji-film Electronic materials) was used as a substrate material and provided excellent physical and electrical properties [15, 16]. Figure 1(b) shows a schematic diagram of the PI electrode preparation process. Titanium (Ti) (30 nm) and gold (Au) (50 nm) were deposited as sacrificial layers on the Si wafer using an e-beam evaporator. The first PI layer was spin-coated (1500 rpm) on the sacrificial layer and was soft-baked on a $100\ ^\circ\text{C}$ hotplate for 3 min. The via-hole of the soft-baked first PI layer was fabricated by exposure to UV light (length: $365\ \text{nm}$, energy: $110\ \text{mJ cm}^{-2}$) through a mask, followed by developing and rinsing processes. The first metal layer (Ti/Au = 30/100 nm thickness) was deposited using an e-beam evaporator, and the recording sites, interconnection pads and interconnection lines were patterned following reported wet metal etching processes [17]. Onto the metal

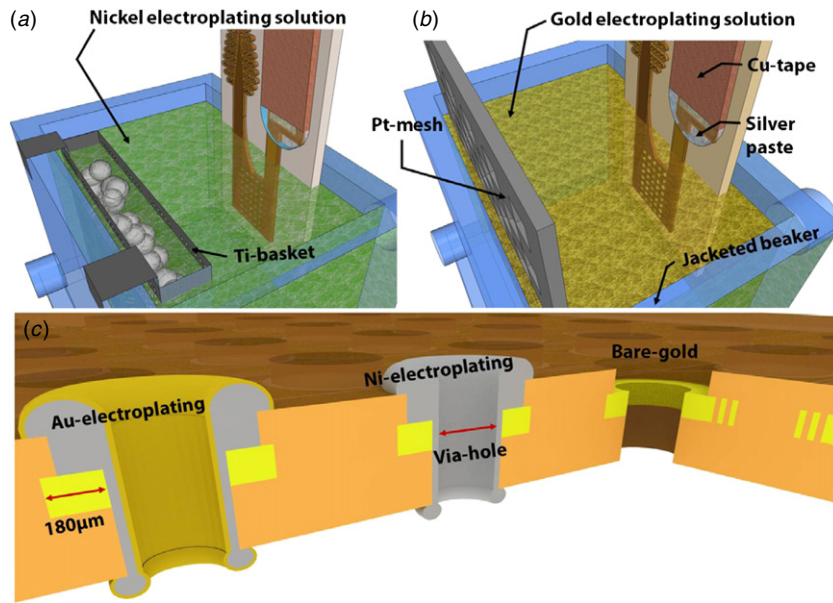


Figure 2. A schematic diagram of the nickel (a) and gold electroplating baths (b). (c) A cross-sectional schematic diagram showing a bare gold, electroplated nickel and the electroplated gold structure.

patterns, the second PI layer was spin-coated, followed by soft-baking to passivate the metal line. The recording sites and interconnection pads (figure 1(e)) were exposed by a wet PI etching process, and then hard-baked. The completed PI electrode was released from the sacrificial layer by dissolving the Au and Ti sacrificial layers using a 0.9% NaCl₂ solution for 3 min at an applied potential of 3 V at room temperature (figure 1(f)) [18].

The interconnection pads were electroplated with nickel and gold (figures 1(g) and (h)). The bypass line was used to electroplate the interconnection pads. The bypass line played a key role in applying the current to the interconnection pads during the electroplating process without significantly damaging the recording sites.

2.2. Electroplating of the interconnection pads

To achieve easy adhesion between the electrode and the PCB connector, we electroplated the connecting pad. A schematic diagram showing the nickel and gold electroplating baths is presented in figures 2(a) and (b). The titanium (Ti) basket containing a nickel source was used as the anode. The PI electrode was fixed on the glass plate using Kapton tape, and the Cu-tape was bonded to the bypass line with the silver paste to apply a constant current (Keithley 2400). A jacketed beaker was used as the bath, and the temperature of the electroplating solution (figure 2(a)) was controlled using a chiller. The chemical compositions of the nickel and gold electroplating solutions are summarized in table 1. All chemicals were purchased from SAMCHUN Chemical, and potassium gold cyanide was purchased from ShinPoong Metal.

Prior to electroplating, the fixed PI electrode on the glass was exposed to oxygen (O₂) plasma (FEMTO Science, CUTE) for 5 min. The surfaces of the plasma-treated interconnection pads were activated with a mixture of PdCl₂ (0.1 g), 30% HCl (0.15 mL) and distilled water (100 mL) [21]. Subsequently,

Table 1. Proportions of nickel and gold in the electroplating solution [19, 20].

Nickel electroplating solution		Gold electroplating solution	
Nickel sulfate	300 g L ⁻¹	Citric acid	80 g L ⁻¹
Nickel chloride	57 g L ⁻¹	Potassium citrate	80 g L ⁻¹
Boric acid	57 g L ⁻¹	Potassium gold cyanide	30 g L ⁻¹
Bath temp.	70 °C	Bath temp.	80 °C
pH	7–8	pH	7

Table 2. Nickel electroplating conditions.

Electroplating time (min)	Current density (A cm ⁻²)		
10			
20	0.25 A cm ⁻²	0.5 A cm ⁻²	1.0 A cm ⁻²
30			

the interconnection pads of the PI electrode were dipped in the nickel electroplating solution for 10, 20 or 30 min, and currents of densities 0.25, 0.5 or 1.0 A cm⁻² were applied, respectively. The Ni electroplating conditions are summarized in detail in table 2. After Ni electroplating, the interconnection pads were electroplated with a gold thin layer (figure 2(b)). After completion of the electroplating process, the bypass line was incised with a sharp razor.

Figure 2(c) shows a cross-sectional schematic diagram of the electroplated structure. Initially, the gold layer was patterned by e-beam evaporator deposition and wet etching to prepare a seed layer for the electroplating process. During the Ni electroplating, a thick Ni layer grew rapidly through the seed layer of the PI electrode, and the doughnut shape of the Ni structure was created on either side of the via-holes by the over-growth of Ni. Finally, a thin gold (2 µm) layer was electroplated to enhance the wettability of the solder.

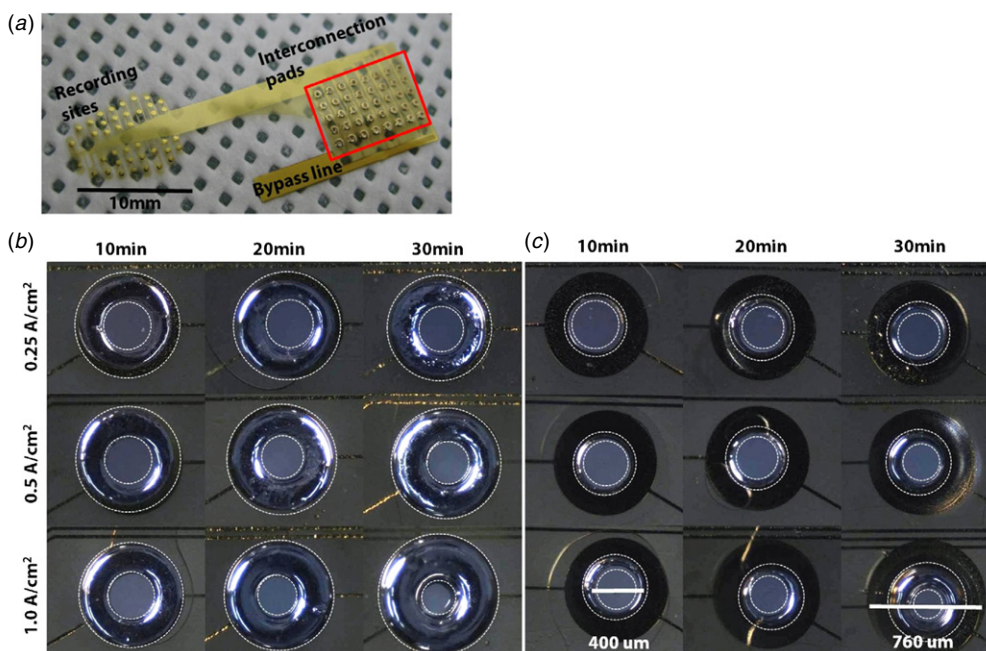


Figure 3. The illustrated optical images show the arrayed PI electrode fabricated via-hole using photolithographic processes. (a) The fabrication process was successful. (b) The magnified optical image of the electroplated nickel ring shows the front-side view. (c) The optic image shows the formation of a Ni ring at the backside view.

2.3. Characterization of the electrical properties

The packaging method was evaluated by measuring the resistance changes at the interconnection pad using a digital multimeter (Agilent 34401A, Agilent Technologies, USA). The electrochemical impedance spectroscopy (EIS) of the completely packaged PI electrodes was measured using a potentiostat with a commercial software package (Gamry Instruments, EIS300™). A solution of 1 M phosphate buffered saline (PBS, pH = 7.4) was used as the electrolyte solution at room temperature. The Ag/AgCl electrode was used as a reference electrode, and a coiled platinum wire was used as a counter electrode. The ac sinusoidal signal with 10 mV root-mean-square amplitude and a frequency range from 1 Hz to 100 kHz was used as the input signal.

2.4. Animal tests

As a demonstration of the connection method, 32-channel evoked potential signals were recorded simultaneously from the skull of a rat. For the surgery, deep anesthesia was induced by injection of a 20% diluted urethane solution (1.5 g kg^{-1} , i.p., Sigma-Aldrich Co.). The animal was mounted on a stereotaxic apparatus, and the middle scalp was incised about 3 cm. The periosteum was removed using cotton swabs without damaging the surrounding tissues. The PI electrode was positioned from AP = -2.5 to 6.5 (AP: anterior posterior). The gold screw electrode with a diameter of 2 mm was placed on AP = 1.5, L = 7.5 for the reference electrode (figures 8(a) and (b)), and the ground electrode was placed at the tail. For electrical stimulation, the bipolar electrodes were fixed at the left hind paw with an inter-electrode distance of 10 mm. The positive current pulses of 4 mA were applied with pulse wave (stimuli time 100 ms, resting time 5 s) for 30 s as

shown in figure 8(c). The somatosensory evoked potential (SEP) was recorded (sampling rate: 512 Hz) from the skull using fabricated PI electrodes with an LXE3232-RF amplifier (LAXTHA, Inc., Korea) and the measured data were analyzed using Matlab.

3. Results and discussion

3.1. Design and fabrication of the polyimide electrode

Figure 3(a) illustrates the arrayed PI electrodes fabricated using photolithographic processes. The fabrication process was successful. The thickness of the PI electrode was $10 \mu\text{m}$, and the diameters of each interconnection pad and via-hole were 760 and $400 \mu\text{m}$, respectively. Figure 3(b) shows a magnified image of the electroplated Ni from a top view, and the thicker electroplated ring structures were observed as the current density increased. As predicted in the electroplating scheme shown in figure 2(c), the electroplated Ni ring grew along the seed layer on the interconnection pads. Although the seed layer was not deposited on the surface of the via-hole and on the backside of the PI electrode, the electroplated Ni ring on the backside of the PI electrode formed by the over-growth of Ni. The electroplating time played a key role in tuning this overgrowth. Figure 3(c) shows the formation of a Ni ring at the backside of the PI electrode as a function of the electroplating time. Such over-growth enabled the Ni ring to be firmly fixed onto the via-hole and firmly bonded to the PCB using even a manual soldering iron.

We quantitatively measured the thickness of the electroplated Ni rings as a function of the current density and electroplating time. The thickness of the ring was measured using a thickness gauge (ABSOLUTE Digimatic Indicator

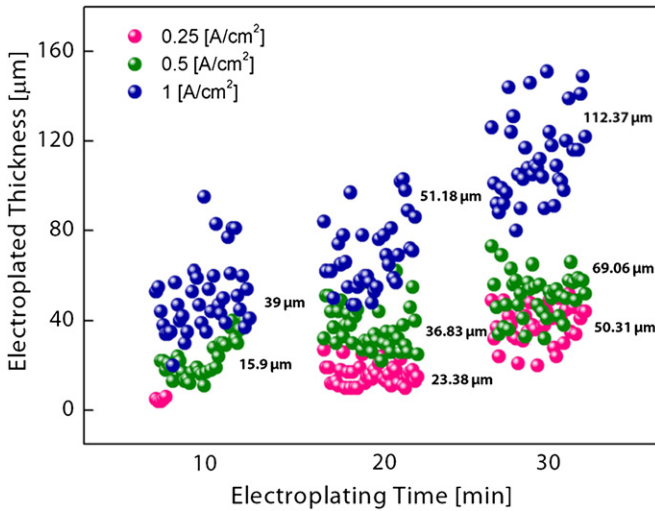


Figure 4. The graph represents the quantitative measurements of the thickness of the electroplated Ni rings as a function of the current density and electroplating time.

ID-C Series 543, Mitutoyo), and the results are plotted in figure 4. As predicted, the thickness of the Ni ring increased with the current density and the electroplating time, and was more sensitive to the electroplating time than to the current density. Considering the thickness and shape of the electroplated ring on the surfaces of the front- and backsides, 0.5 A cm⁻² and 30 min electroplating conditions were most suitable for subsequent applications. The ring structure

prepared under these conditions was closely inspected by SEM imaging, and the results are shown in figure 5. Figures 5 (a) and (b) present SEM images of the well-grown Ni ring on the front and back surfaces. The cross-sectional view of the interconnection pad clearly shows the electroplated ring structure (figures 5(c) and (d)). As shown in the dotted-red circle, the thin interconnection pads of the PI layer were caught by both the front and back rings, which protected the thin PI layer from thermal damage during the soldering process and facilitated strong adhesion to the PCB board. The dotted-blue rectangle indicates the surface of the via-hole, and the over-growth of Ni across the via-hole is clearly observed.

3.2. Assembly and packaging

After the Ni electroplating process, which formed the Ni ring, gold was electroplated onto the surface of the electroplated nickel to improve the wettability of the eutectic solder and to facilitate penetration of the solder into the via-holes of both the electrode and the PCB. The thin PI electrode was bonded to the PCB by aligning the electroplated via-hole of the electrode with the through-holes of the PCB (figure 6(a)—top). The aligned PI electrode and PCB were bonded by soldering (figure 6(a)—bottom). Even the manual soldering process was easily performed. Figure 6(b) shows a photograph of a completely packaged PI electrode. The female connector was used for the connection to the amplifier. Figure 6(c) shows the interconnection pads of the electrode, from the front- and backsides, and figure 6(d) shows the

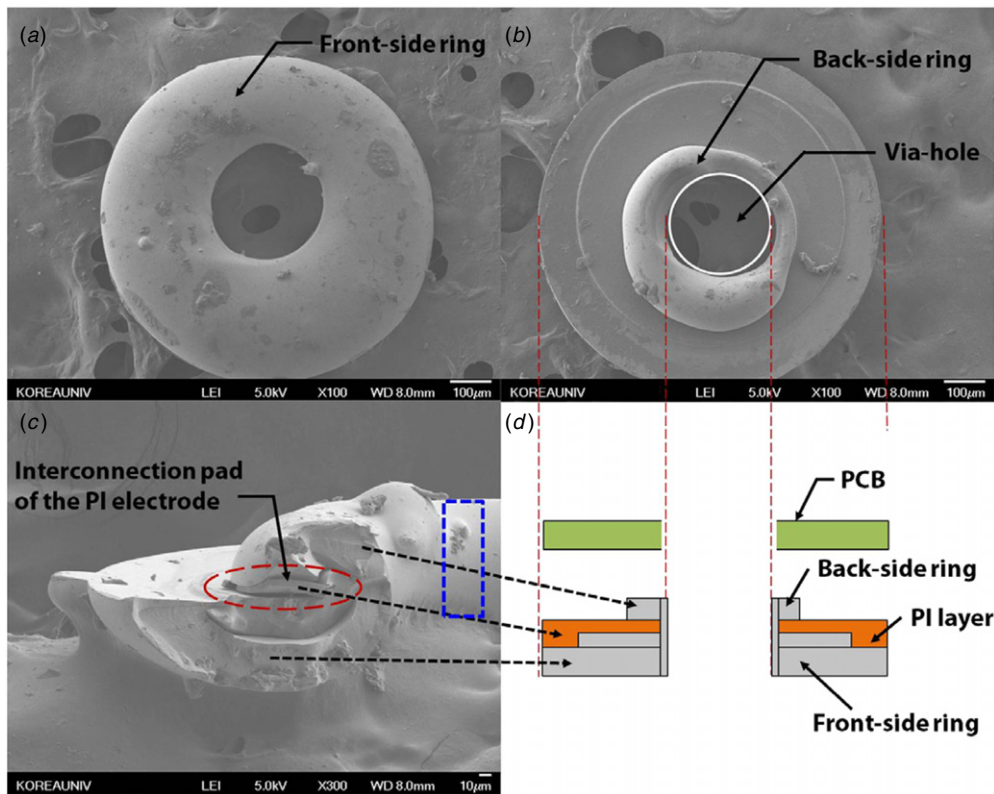


Figure 5. SEM images of the electroplated nickel ring on the interconnection pad. (a) The front-side surface. (b) The backside surface. (c) The cross-section of the interconnection pad and nickel ring. (d) Schematic diagram of the electroplated structure and assembly with the PCB.

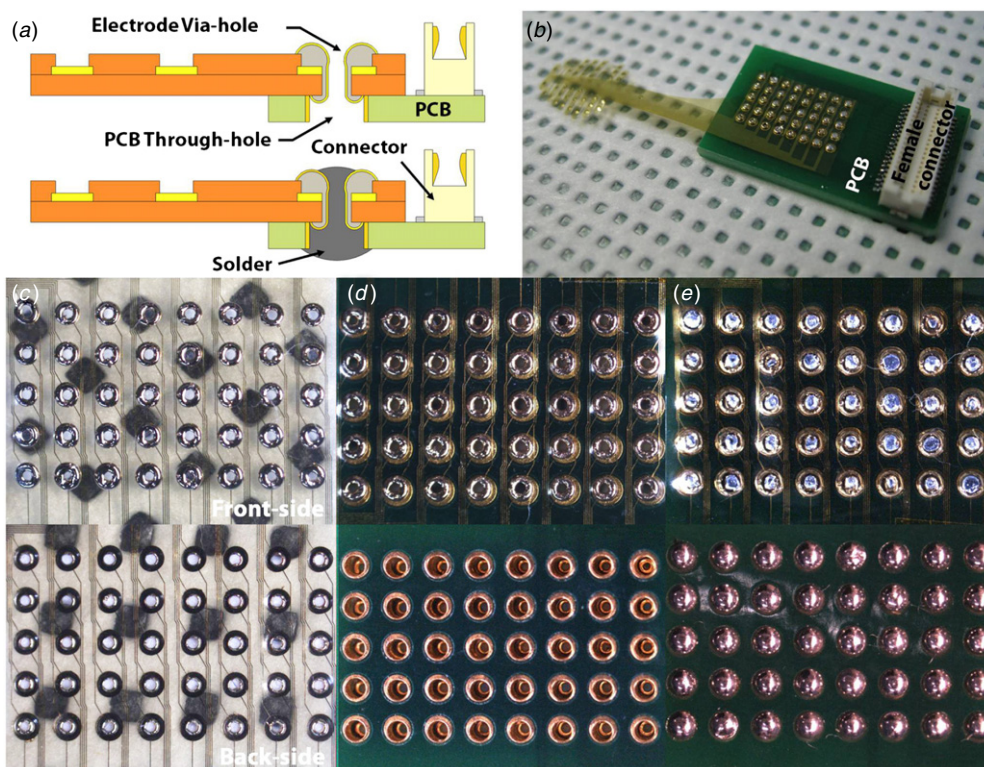


Figure 6. The plot illustrates the magnitude of impedance (ohm) and phase (degree) of the fully packaged PI electrode and these values were measured with the electrochemical impedance spectroscopy measurement.

interconnection pads aligned to the PCB, from both sides. The aligned interconnection pads were soldered using soldering iron. Figure 6(e) shows the front- and backside views of the soldered interconnection pads. The melted solder successfully penetrated both via-holes and bonded to both the electrode and the PCB. The packaging process for the interconnection pads yielded an electrical connection success rate of more than 99%, and damage to the PI electrode during the soldering process was not observed. The mechanical robustness was simply tested by manual pulling of the electrode horizontally until the electrode was broken. Tests of ten samples revealed that the breakage or disconnection was not observed at the interconnection pads. These results demonstrate that the proposed soldering method is sufficiently robust to endure harsh environments, and it will be useful in devices that must tolerate a large degree of motion.

3.3. Resistance and electrochemical impedance measurements

We measured the resistance changes before and after electrical connection to the PCB. The resistance change rate $((R_{\text{after}} - R_{\text{before}}) / R_{\text{before}})$ was approximately $1.3\% \pm 1.1$ and the average of R_{before} and R_{after} is $1.856 \pm 0.03 \Omega$ and $1.860 \pm 0.017 \Omega$, respectively. This value indicated that the proposed electrical connection method did not significantly reduce the electrical conductance. The impedance of the fully packaged PI electrode was characterized, and the impedance magnitude (|ZI|) and phase (degree) are plotted in figure 7. The magnitude at 100 Hz was $40.8 \text{ k}\Omega \pm 10.3 \text{ k}\Omega$ (mean \pm SD), and

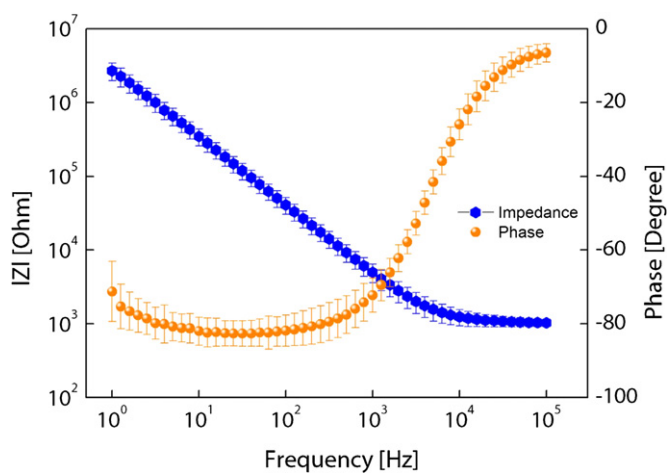


Figure 7. (a—top) The electroplated via-holes of the electrodes were aligned to the through-holes of the PCB; (a—bottom) the aligned PI electrode and PCB were bonded by soldering. (b) Photograph of a completely packaged PI electrode. (c) The interconnection pads of the electrode show from the frontside and backsides. (d) The images indicate the interconnection pads aligned with the PCB, from both sides. (e) The aligned interconnection pads were soldered, as shown in the frontside and backside views of the soldered interconnection pads and the melted solder.

100 Hz is the biologically relevant frequency for neural activity [22]. The phase plot indicated that the phase was $-81.8^\circ \pm 4.2^\circ$ at 100 Hz. The impedance magnitude covered a range similar to that seen in comparisons with other electrodes [23–25], indicating that the proposed connection method did not significantly affect the electrode performance. The

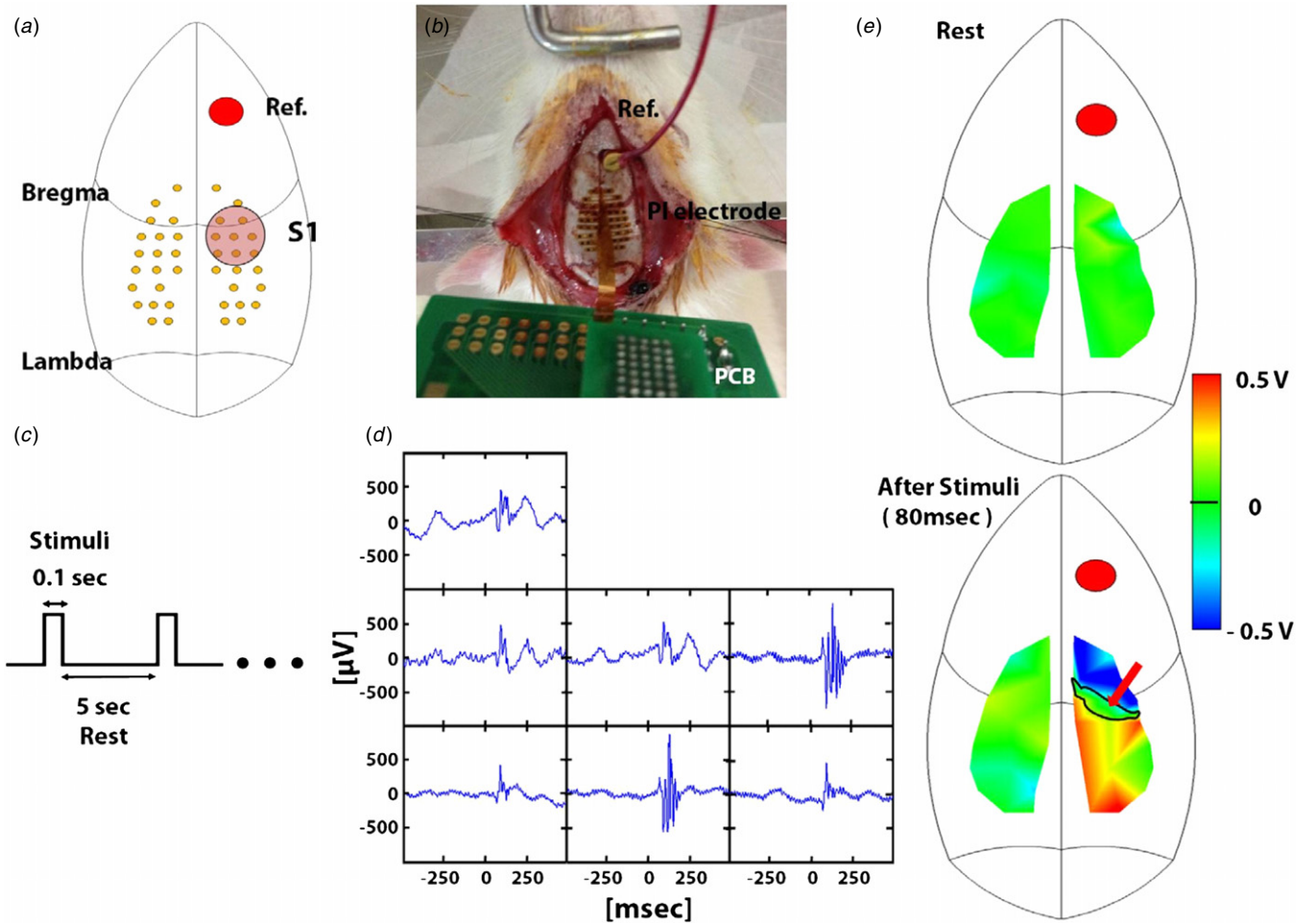


Figure 8. (a), (b) The images show the PI electrode placed on the primary somatosensory cortex (S1) of the rat’s skull. (c) The amplitude of the 4 mA current applied with the pulse wave (stimulus time 100 ms, resting time 5 s). (d) The evoked signals from seven channels on the S1 area. (e) Somatosensory evoked potential was recorded at the primary sensory area of the skull before and after hind paw stimulation.

packaged PI electrode was therefore shown to be useful for measuring bio-signals, especially, neural signals.

3.4. Animal tests

The proposed connection method was validated by fabricating a 40-channel PI electrode and packaging it with the PCB, including the female connector. The electrode was placed on the skull of a rat, and the evoked potential was measured by electrical stimulation as shown in figure 8(c). The anatomy of the rat brain in figure 8(a) presents the location of the primary somatosensory cortex (S1) on the rat skull. The S1 area is a critical area, the anatomy and synaptic physiology of which are designed to guide in exploring the environment [26, 27]. Figure 8(b) shows a PI electrode that was placed on the skull of a rat. To further confirm the reliability of neural signal recordings, we evaluated the signal-to-noise ratio (SNR) of the recorded SEPs. The SNR was defined as the ratio of powers between SEPs and a baseline neural activity recorded before the electrical stimulation of the hind paw. The baseline signals were acquired from 1 s intervals before the stimulation onset, and their average powers were evaluated for each electrode. The ‘signal’ interval was defined as the 250 ms interval from the stimulus onset as the interval

generally included main SEP peaks as shown in figure 8(d). The SNR value averaged over all channels was 9.52 dB and the highest SNR among all channel SNRs reached to 16.86 dB, which is obviously a very high SNR value considering that we did not apply any ensemble averaging over the test trials. Each recording electrode measured electrical brain activity response successfully. The recorded SEP of the right hemisphere electrical activity indicates that the evoked potentials were activated by electrical stimulation. Figure 8(e) represents the topo-plot of evoked potential signals in the resting and stimulated state and the positive and negative potentials on the right hemisphere. Commonly, the EEG source is localized in the middle of the of the peak position arising from the positive and negative potential. The SEP was generated at the equivalent source location with an EEG source. The roughly estimated neural source location coincided well with the known anatomical location of the primary somatosensory cortex of hind limb [28]. Consequently, the result involves that the proposed packaging method approach does not negatively affect the signal measurement and our system can reliably record neural signal without significant contamination of the signal.

4. Conclusions

The construction of a Ni ring through a via-hole successfully provided a highly yieldable, stable and cost-effective packaging procedure. And we designed the bypass line for electroplating on the interconnection pads to form the Ni ring of uniform thickness. The packaging method is easy that the electrical connections between the thin PI electrode and the PCB were made by manual soldering. The electrical characterization demonstrated that the solder bonded between the interconnection pads of the PI electrode and PCB strongly and the resistance was negligible before and after electrically connected with the PCB. The *in vivo* tests demonstrated that the average channel SNR was 9.52 dB and the packaged PI electrode could measure the SEP on the rat skull by electrical stimulation at the hind paw. This packaging method could be used for the continuous measurement of bio-signals or in neural prosthetics.

Acknowledgments

This research was supported by the Public Welfare & Safety Research Program through the National Research Foundation of Korea (NRF) funded by the Ministry of Education, Science and Technology (20110020943) and this study was supported by a grant of the Korean Health Technology R&D Project, Ministry of Health and Welfare, Republic of Korea (A092052).

References

- [1] Donoghue J P 2002 Connecting cortex to machines: recent advances in brain interfaces *Nature Neurosci.* **5** 1085–88
- [2] Chapin J K, Moxon K A, Markowitz R S and Nicolelis M A L 1999 Real-time control of a robot arm using simultaneously recorded neurons in the motor cortex *Nature Neurosci.* **2** 664–70
- [3] Velliste M, Perel S, Spalding M C, Whitford A S and Schwartz A B 2008 Cortical control of a prosthetic arm for self-feeding *Nature* **453** 1098–101
- [4] Kalaska J F 2008 Neuroscience: brain control of a helping hand *Nature* **453** 994–95
- [5] Meyer J, Stieglitz T, Scholz O, Haberer W and Beutel H 2001 High density interconnects and flexible hybrid assemblies for active biomedical implants *IEEE Trans. Adv. Packag.* **24** 366–74
- [6] Stieglitz T, Schuetter M and Koch K 2005 Implantable biomedical microsystems for neural prostheses *IEEE Eng. Med. Biol. Mag.* **24** 58–65
- [7] Stieglitz T, Beutel H, Schuetter M and Meyer J U 2000 Micromachined, polyimide-based devices for flexible *Neural Interfaces Biomed. Microdevices* **2** 283–94
- [8] Birthe R, Conrado B, Robert O, Pascal F and Thomas S 2009 A MEMS-based flexible multichannel ECoG-electrode array *J. Neural Eng.* **6** 036003
- [9] Patrick E, Sankar V, Rowe W, Sanchez J C and Nishida T 2009 Design of an implantable intracortical microelectrode system for brain-machine interfaces *4th Int. IEEE/EMBS Conf. on Neural Engineering* pp 379–82
- [10] Huang R *et al* 2008 Integrated parylene-cabled silicon probes for neural prosthetics *MEMS 2008: IEEE 21st Int. Conf. on Micro Electro Mechanical Systems* pp 240–43
- [11] Gutierrez C A, Lee C, Kim B and Meng E 2011 Epoxy-less packaging methods for electrical contact to parylene-based flat flexible cables *16th Int. Solid-State Sensors Actuators and Microsystems Conf. (TRANSDUCERS)* pp 2299–302
- [12] Myllymaa S *et al* 2009 Fabrication and testing of polyimide-based microelectrode arrays for cortical mapping of evoked potentials *Biosensors Bioelectron.* **24** 3067–72
- [13] Baek D H *et al* 2011 Interconnection of multichannel polyimide electrodes using anisotropic conductive films (ACFs) for biomedical applications *IEEE Trans. Biomed. Eng.* **58** 1466–73
- [14] Kim D-H *et al* 2010 Dissolvable films of silk fibroin for ultrathin conformal bio-integrated electronics *Nature Mater.* **9** 511–17
- [15] Richardson R R Jr, Miller J A and Reichert W M 1993 Polyimides as biomaterials: preliminary biocompatibility testing *Biomaterials* **14** 627–35
- [16] Boppart S A, Wheeler B C and Wallace C S 1992 A flexible perforated microelectrode array for extended neural recordings *IEEE Trans. Biomed. Eng.* **39** 37–42
- [17] Baek D H *et al* 2011 A dry release of polyimide electrodes using Kapton film and application to EEG signal measurements *Microsyst. Technol.* **17** 7–14
- [18] Metz S, Bertsch A and Renaud P 2005 Partial release and detachment of microfabricated metal and polymer structures by anodic metal dissolution *J. Microelectromech. Syst.* **14** 383–91
- [19] Yoshida H *et al* 2003 Application of emulsion of dense carbon dioxide in electroplating solution with nonionic surfactants for nickel electroplating *Surf. Coat. Technol.* **173** 285–92
- [20] Duva R 1968 (inventor) SEL REX CORP (assignee) *Chemical Gold Plating Composition Patent* US3396042
- [21] Wang L C, Huang C Y, Chang C Y, Lin W C and Chao K J 2008 Formation of Pd nanoparticles in surfactant-mesoporous silica composites and surfactant solutions *Microporous Mesoporous Mater.* **110** 451–60
- [22] Mercanzini A, Colin P, Bensadoun J C, Bertsch A and Renaud P 2009 *In vivo* electrical impedance spectroscopy of tissue reaction to microelectrode arrays *IEEE Trans. Biomed. Eng.* **56** 1909–18
- [23] Fomani A A, Mansour R R, Florez-Quenguan C M and Carlen P L 2011 Development and characterization of multisite three-dimensional microprobes for deep brain stimulation and recording *J. Microelectromech. Syst.* **20** 1109–18
- [24] Takahashi H, Ejiri T, Nakao M, Nakamura N, Kaga K and Herve T 2003 Microelectrode array on folding polyimide ribbon for epidural mapping of functional evoked potentials *IEEE Trans. Biomed. Eng.* **50** 510–16
- [25] Choi J H, Koch K P, Poppendieck W, Lee M and Shin H-S 2010 High resolution electroencephalography in freely moving mice *J. Neurophysiol.* **104** 1825–34
- [26] Feldman D E and Brecht M 2005 Map plasticity in somatosensory cortex *Science* **310** 810–15
- [27] Sanchez-Jimenez A, Panetsos F and Murciano A 2009 Early frequency-dependent information processing and cortical control in the whisker pathway of the rat: electrophysiological study of brainstem nuclei principalis and interpolaris *Neuroscience* **160** 212–26
- [28] Hjørnevik T *et al* 2007 Three-dimensional atlas system for mouse and rat brain imaging data *Front. Neuroinform.* **1** 4